AMERICAN NUCLEAR SOCIETY

555 North Kensington Avenue
La Grange Park, Illinois
60526-5592 USA

Tel: 708 / 352-6611
E-Mail: NUCLEUS@ans.org
http: //www.ans.org
Fax: 708 / 352-0499

AUTHOR PROOF INSTRUCTIONS

Your paper is scheduled for publication in a forthcoming issue of *Nuclear Science and Engineering*. You are receiving your author proofs electronically. You will not receive anything in the regular mail. Please follow these procedures:

1. Download your author proof, print it out, and review it.

2. Proofread your paper very carefully. This will be your final reading before publication. This material has been copyedited and typeset from the disk/electronic file that you provided with your manuscript or from the hard copy that you provided, and it has been transmitted to you through the Internet. This process produces excellent results, but please check the following especially carefully: translation of Greek letters, accented letters, special characters, superscripts and subscripts, and mathematical symbols; typesetting of mathematics; and formatting of tables. Also, note that your manuscript has been copyedited according to ANS technical journal style; please check that technical meanings have been unaffected by the copyediting. Please limit your corrections to those that are absolutely necessary because changes at this stage of processing are both time-consuming and expensive.

3. Please note that the typesetter has used low-resolution electronically scanned versions of your figures as FPOs (for position only). These will be replaced with high-resolution versions at the printing stage.

4. Necessary corrections should be sent as follows: (a) a list of corrections sent by electronic mail and/or (b) your manuscript with your corrections marked on it sent by fax (your fax should include a list of your corrections). If you have been sent a list of queries, we would greatly appreciate your reply to these queries either by electronic mail or by fax.

5. Please return your corrections within a week of receipt of your author proofs. Note that delay in transmitting your corrections may delay publication of your paper or may require publication without your corrections.

6. Return proofs using the following name and electronic mail address or fax number:

Suzanne Pals
E-mail: spals@ans.org
Fax: 708-352-6464

Thank you for your prompt attention to these proofs. If you have any questions, please feel free to contact me.

Suzanne Pals
Staff Editor

NUCLEAR SCIENCE AND ENGINEERING: **149**, 1–8 (2005)

Modified Nodal Integral Method for the Three-Dimensional, Time-Dependent, Incompressible Navier-Stokes Equations

Fei Wang and Rizwan-uddin*

University of Illinois at Urbana-Champaign
Department of Nuclear, Plasma and Radiological Engineering
103 S. Goodwin Avenue, Urbana, Illinois 61801

Received January 30, 2004
Accepted August 9, 2004

Abstract—*A modified nodal integral method (MNIM) for two-dimensional, time-dependent Navier-Stokes equations is extended to three dimensions. The nodal integral method is based on local transverse integrations over finite size cells that reduce each partial differential equation to a set of ordinary differential equations (ODEs). Solutions of these ODEs in each cell for the transverse-averaged dependent variables are then utilized to develop the difference schemes. The discrete variables are scalar velocities and pressure, averaged over the faces of bricklike cells. The development of the MNIM is different from the conventional nodal method in two ways: (a) it is Poisson-type pressure equation based and (b) the convection terms are retained on the left side of the transverse-integrated equations and thus contribute to the homogeneous part of the solution. The first feature leads to a set of symmetric transverse-integrated equations for all the velocities, and the second feature yields distributions of constant + linear + exponential form for the transverse-averaged velocities. The scheme is tested on three-dimensional lid-driven cavity problems in cube- and prism-shaped cavities. Results obtained using the MNIM on fairly coarse meshes are comparable with reference solutions obtained using much finer meshes.*

I. INTRODUCTION

Nodal methods have been developed over the last two decades to solve the Navier-Stokes (N-S) equations.[1–5] Recent developments of nodal integral methods (NIMs) for fluid flow problems show improvements in efficiency over more conventional approaches similar to those shown by nodal methods developed for neutronics problems. (A review of nodal methods developed in the nuclear industry is given by Lawrence.[6]) Applying coarse mesh methods to the N-S equations promises solution of much larger scale fluid dynamics problems as well as direct numerical simulation of turbulent flow. A two-dimensional (2-D) modified NIM (MNIM) has been developed recently[5] with two new features: (a) a Poisson-type pressure equation was used instead of the continuity equation and (b) convection terms in the N-S equations are kept on the left side and thus contribute to the homogeneous solution of the transverse-integrated ordinary differential equations (ODEs). Here, we extend the 2-D MNIM to three dimensions. The extension is straightforward but not trivial.

Usually, the NIM is limited to a domain with boundaries parallel to one of the Cartesian axes. However, recently, NIMs have been extended to arbitrary geometries.[7] A similar approach can be used to develop the MNIM for the three-dimensional (3-D) N-S equations for arbitrary geometries.

A note on terminology: Since the term "node" is in high demand (in the NIM, it is used to represent a finite volume in the space of independent variables, it represents a point in space in finite difference and finite volume methods, and it is also used to represent a processor or a group of processors for parallel computation of computational fluid dynamics problems), in this paper we will use the term "cell" to denote what was called a "node" by Azmy and Dorning[1] when they developed their NIM for the N-S equations.

*E-mail: rizwan@uiuc.edu

II. DEVELOPMENT OF THE MODIFIED NODAL INTEGRAL METHOD

II.A. Reformulation of the Navier-Stokes Equations

The time-dependent, incompressible N-S equations are

$$\frac{\partial u}{\partial X}+\frac{\partial \mathrm{v}}{\partial Y}+\frac{\partial w}{\partial Z}=0 \tag{1}$$

$$\frac{\partial u}{\partial T}+u\frac{\partial u}{\partial X}+\mathrm{v}\frac{\partial u}{\partial Y}+w\frac{\partial u}{\partial Z}-\upsilon\left[\frac{\partial^2 u}{\partial X^2}+\frac{\partial^2 u}{\partial Y^2}+\frac{\partial^2 u}{\partial Z^2}\right]+\frac{1}{\rho}\frac{\partial p}{\partial X}-g_X(X,Y,Z,T)=0 \tag{2}$$

$$\frac{\partial \mathrm{v}}{\partial T}+u\frac{\partial \mathrm{v}}{\partial X}+\mathrm{v}\frac{\partial \mathrm{v}}{\partial Y}+w\frac{\partial \mathrm{v}}{\partial Z}-\upsilon\left[\frac{\partial^2 \mathrm{v}}{\partial X^2}+\frac{\partial^2 \mathrm{v}}{\partial Y^2}+\frac{\partial^2 \mathrm{v}}{\partial Z^2}\right]+\frac{1}{\rho}\frac{\partial p}{\partial Y}-g_Y(X,Y,Z,T)=0 \tag{3}$$

$$\frac{\partial w}{\partial T}+u\frac{\partial w}{\partial X}+\mathrm{v}\frac{\partial w}{\partial Y}+w\frac{\partial w}{\partial Z}-\upsilon\left[\frac{\partial^2 w}{\partial X^2}+\frac{\partial^2 w}{\partial Y^2}+\frac{\partial^2 w}{\partial Z^2}\right]+\frac{1}{\rho}\frac{\partial p}{\partial Z}-g_Z(X,Y,Z,T)=0\ , \tag{4}$$

where $g(X,Y,Z,T)$ represents volumetric sources such as gravity and capital letters X, Y, Z, and T are used to denote the global coordinates. To develop a numerical scheme, very often a Poisson equation for pressure is used instead of the continuity equation. Manipulating Eqs. (2), (3), and (4), the Poisson equation for pressure is given by[8]

$$\frac{\partial^2 p}{\partial X^2}+\frac{\partial^2 p}{\partial Y^2}+\frac{\partial^2 p}{\partial Z^2}=-\rho\left[\left(\frac{\partial u}{\partial X}\right)^2+\left(\frac{\partial \mathrm{v}}{\partial Y}\right)^2+\left(\frac{\partial w}{\partial Z}\right)^2\right]-2\rho\frac{\partial u}{\partial Y}\frac{\partial \mathrm{v}}{\partial X}-2\rho\frac{\partial \mathrm{v}}{\partial Z}\frac{\partial w}{\partial Y}-2\rho\frac{\partial w}{\partial X}\frac{\partial u}{\partial Y}+\rho\frac{\partial g_X}{\partial X}+\rho\frac{\partial g_Y}{\partial Y}$$
$$+\rho\frac{\partial g_Z}{\partial Z}-\rho\left[\frac{\partial D}{\partial T}+u\frac{\partial D}{\partial X}+\mathrm{v}\frac{\partial D}{\partial Y}+w\frac{\partial D}{\partial Z}-\upsilon\frac{\partial^2 D}{\partial X^2}-\upsilon\frac{\partial^2 D}{\partial Y^2}-\upsilon\frac{\partial^2 D}{\partial Z^2}\right]\ , \tag{5}$$

where the dilatation term D is given by

$$D\equiv\frac{\partial u}{\partial X}+\frac{\partial \mathrm{v}}{\partial Y}+\frac{\partial w}{\partial Z}\ . \tag{6}$$

Since Eq. (5) was derived only from the momentum equations (2), (3), and (4), the continuity equation can be incorporated into Eq. (5) by simply setting D equal to zero. But, as reported,[8,9] this may cause numerical instability in the scheme. In the MNIM, keeping only the temporal derivative term $\partial D/\partial T$ while setting the other terms in the bracket to zero leads to a stable scheme.

In the nodal method, the space-time domain (X, Y, Z, T) is first discretized into rectangular space-time cells (i, j, k, n) of size ($2a_i \times 2b_j \times 2c_k \times 2\tau_n$) with cell-centered local coordinates ($-a_i \le x \le a_i$, $-b_j \le y \le b_j$, $-c_k \le z \le c_k$, $-\tau_n \le t \le \tau_n$). The N-S equations are rewritten in terms of local coordinates:

$$\frac{\partial u}{\partial t}+u_p\frac{\partial u}{\partial x}+\mathrm{v}_p\frac{\partial u}{\partial y}+w_p\frac{\partial u}{\partial z}-\upsilon\left[\frac{\partial^2 u}{\partial x^2}+\frac{\partial^2 u}{\partial y^2}+\frac{\partial^2 u}{\partial z^2}\right]$$
$$=-\frac{1}{\rho}\frac{\partial p}{\partial x}+g_x(x,y,z,t)-(u-u_p)\frac{\partial u}{\partial x}-(\mathrm{v}-\mathrm{v}_p)\frac{\partial u}{\partial y}-(w-w_p)\frac{\partial u}{\partial z} \tag{7}$$

$$\frac{\partial \mathrm{v}}{\partial t}+u_p\frac{\partial \mathrm{v}}{\partial x}+\mathrm{v}_p\frac{\partial \mathrm{v}}{\partial z}+w_p\frac{\partial \mathrm{v}}{\partial z}-\upsilon\left[\frac{\partial^2 \mathrm{v}}{\partial x^2}+\frac{\partial^2 \mathrm{v}}{\partial y^2}+\frac{\partial^2 \mathrm{v}}{\partial z^2}\right]$$
$$=-\frac{1}{\rho}\frac{\partial p}{\partial y}+g_y(x,y,z,t)-(u-u_p)\frac{\partial \mathrm{v}}{\partial x}-(\mathrm{v}-\mathrm{v}_p)\frac{\partial \mathrm{v}}{\partial y}-(w-w_p)\frac{\partial \mathrm{v}}{\partial z} \tag{8}$$

$$\frac{\partial w}{\partial t}+u_p\frac{\partial w}{\partial x}+\mathrm{v}_p\frac{\partial w}{\partial y}+w_p\frac{\partial w}{\partial z}-\upsilon\left[\frac{\partial^2 w}{\partial x^2}+\frac{\partial^2 w}{\partial y^2}+\frac{\partial^2 w}{\partial z^2}\right]$$
$$=-\frac{1}{\rho}\frac{\partial p}{\partial z}+g_z(x,y,z,t)-(u-u_p)\frac{\partial w}{\partial x}-(\mathrm{v}-\mathrm{v}_p)\frac{\partial w}{\partial y}-(w-w_p)\frac{\partial w}{\partial z} \tag{9}$$

$$\frac{\partial^2 p}{\partial x^2}+\frac{\partial^2 p}{\partial y^2}+\frac{\partial^2 p}{\partial z^2}=-\rho\left[\left(\frac{\partial u}{\partial x}\right)^2+\left(\frac{\partial \mathrm{v}}{\partial y}\right)^2+\left(\frac{\partial w}{\partial z}\right)^2\right]$$
$$-2\rho\frac{\partial u}{\partial y}\frac{\partial \mathrm{v}}{\partial x}-2\rho\frac{\partial \mathrm{v}}{\partial z}\frac{\partial w}{\partial y}-2\rho\frac{\partial w}{\partial x}\frac{\partial u}{\partial y}+\rho\frac{\partial g_X}{\partial x}+\rho\frac{\partial g_Y}{\partial y}+\rho\frac{\partial g_Z}{\partial z}-\rho\frac{\partial D}{\partial t}\ , \tag{10}$$

where u_p, v_p, and w_p are the cell-averaged u, v, and w velocities, respectively, at the previous time step.[5] Equations (7), (8), and (9) are different from the standard momentum equations [Eqs. (2), (3), and (4)] in that convection terms based on cell-averaged velocities at the previous time step have been added on both sides of the equations and the original convection terms are moved to the right side. The reason behind writing the momentum equations in this form is to reduce the computational burden that results if the nonlinearity of the convection term (at the current time step) is resolved iteratively.[5]

II.B. Transverse Integration Procedure

Time, in this modified nodal scheme, is treated in the same fashion as spatial coordinates. By applying the local transverse integration procedure, such as

$$\bar{\phi}^{xyt}_{i,j,k,n}(z) \equiv \frac{1}{8a_i b_j \tau_n}\int_{-\tau_n}^{\tau_n}\int_{-b_j}^{b_j}\int_{-a_i}^{a_i}\phi_{i,j,k}(x,y,z,t)\,dxdydt \ , \qquad \phi = u, v, w, p \ , \tag{11}$$

to Eqs. (7) through (10), one obtains 15 transverse-integrated ODEs:

$$\frac{d^2\bar{p}^{yzt}(x)}{dx^2} = \bar{S}_1^{yzt}(x) \ , \tag{12}$$

$$\frac{d^2\bar{p}^{zxt}(y)}{dy^2} = \bar{S}_1^{zxt}(y) \ , \tag{13}$$

$$\frac{d^2\bar{p}^{xyt}(z)}{dz^2} = \bar{S}_1^{xyt}(z) \ , \tag{14}$$

$$u_p\frac{d\bar{u}^{yzt}(x)}{dx} - v\frac{d^2\bar{u}^{yzt}(x)}{dx^2} = \bar{S}_2^{yzt}(x) \ , \tag{15}$$

$$u_p\frac{d\bar{v}^{yzt}(x)}{dx} - v\frac{d^2\bar{v}^{yzt}(x)}{dx^2} = \bar{S}_3^{yzt}(x) \ , \tag{16}$$

$$u_p\frac{d\bar{w}^{yzt}(x)}{dx} - v\frac{d^2\bar{w}^{yzt}(x)}{dx^2} = \bar{S}_4^{yzt}(x) \ , \tag{17}$$

$$v_p\frac{d\bar{u}^{zxt}(y)}{dy} - v\frac{d^2\bar{u}^{zxt}(y)}{dy^2} = \bar{S}_2^{zxt}(y) \ , \tag{18}$$

$$v_p\frac{d\bar{v}^{zxt}(y)}{dy} - v\frac{d^2\bar{v}^{zxt}(y)}{dy^2} = \bar{S}_3^{zxt}(y) \ , \tag{19}$$

$$v_p\frac{d\bar{w}^{zxt}(y)}{dy} - v\frac{d^2\bar{w}^{zxt}(y)}{dy^2} = \bar{S}_4^{zxt} \ , \tag{20}$$

$$w_p\frac{d\bar{u}^{xyt}(z)}{dz} - v\frac{d^2\bar{u}^{xyt}(z)}{dz^2} = \bar{S}_2^{xyt}(z) \ , \tag{21}$$

$$w_p\frac{d\bar{v}^{xyt}(z)}{dz} - v\frac{d^2\bar{v}^{xyt}(z)}{dz^2} = \bar{S}_3^{xyt}(z) \ , \tag{22}$$

$$w_p\frac{d\bar{w}^{xyt}(z)}{dz} - v\frac{d^2\bar{w}^{xyt}(z)}{dz^2} = \bar{S}_4^{xyt}(z) \ , \tag{23}$$

$$\frac{d\bar{u}^{xyz}(t)}{dt} = \bar{S}_2^{xyz}(t) \ , \tag{24}$$

$$\frac{d\bar{v}^{xyz}(t)}{dt} = \bar{S}_3^{xyz}(t) \ , \tag{25}$$

and

$$\frac{d\bar{w}^{xyz}(t)}{dt} = \bar{S}_4^{xyz}(t) \ , \tag{26}$$

where the subscripts (i, j, k, n) on independent variables have been omitted and terms not explicit are lumped into the right side as pseudo source terms. For example,

$$\bar{S}_1^{zxt}(y) \equiv -\frac{1}{8c_k a_i \tau_n}\int_{-\tau_n}^{\tau_n}\int_{-a_i}^{a_i}\int_{-c_k}^{c_k} dzdxdt \begin{pmatrix} -\dfrac{\partial^2 p}{\partial x^2} - \dfrac{\partial^2 p}{\partial z^2} - \rho\left[\left(\dfrac{\partial u}{\partial x}\right)^2 + \left(\dfrac{\partial v}{\partial y}\right)^2 + \left(\dfrac{\partial w}{\partial z}\right)^2\right] \\ -2\rho\,\dfrac{\partial u}{\partial y}\,\dfrac{\partial v}{\partial x} - 2\rho\,\dfrac{\partial v}{\partial z}\,\dfrac{\partial w}{\partial y} - 2\rho\,\dfrac{\partial w}{\partial x}\,\dfrac{\partial u}{\partial y} \\ +\rho\,\dfrac{\partial g_X}{\partial x} + \rho\,\dfrac{\partial g_Y}{\partial y} + \rho\,\dfrac{\partial g_Z}{\partial z} - \rho\,\dfrac{\partial D}{\partial t} \end{pmatrix} . \tag{27}$$

Notice that the transverse-integrated equations (12) through (26) are similar in form to those obtained in the 2-D MNIM (Ref. 5).

II.C. Local Solutions for the Transverse-Integrated Ordinary Differential Equations

The ODEs are solved analytically within each cell. Particular solutions are obtained after expanding and truncating the modified pseudosource terms at the zeroth order. (In general, truncating at higher order, in conjunction with other consistent approximations, leads to a numerical scheme of order higher than second.) The local solutions

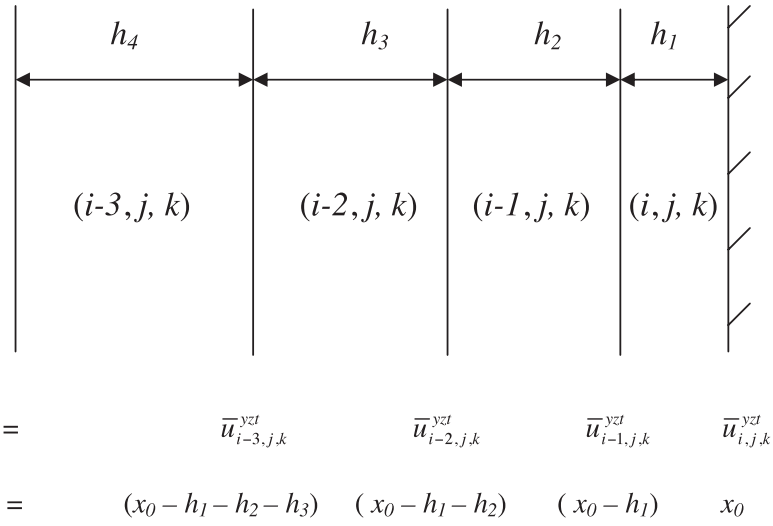

Fig. 1. Boundary condition for pressure at the surface $x = x_{max} = x_0$.

of the ODEs for transverse-integrated pressure are quadratic, and for example, the solution for $\bar{p}^{zxt}(y)$ is given by

$$\bar{p}^{zxt}(y) = \frac{\bar{S}_1^{zxt}}{2} y^2 + C_1 y + C_2 \ . \tag{28}$$

The local solution for $\bar{u}^{zxt}(y)$ is of the following form:

$$\bar{u}^{zxt}(y) = \bar{S}_2^{zxt} e^{v_p y/\upsilon} + C_3 y + C_4 \ . \tag{29}$$

Solutions for the other transverse-integrated velocities $[\bar{u}^{yzt}(x), \bar{u}^{xyt}(z), \bar{v}^{yzt}(x), \bar{v}^{zxt}(y), \bar{v}^{xyt}(z), \bar{w}^{yzt}(x), \bar{w}^{zxt}(y),$ and $\bar{w}^{xyt}(z)]$ are of similar forms. The solutions for $\bar{u}^{xyz}(t)$, $\bar{v}^{xyz}(t)$, and $\bar{w}^{xyz}(t)$ are linear in time. The constants C_i $(i = 1,2,\ldots)$ are eliminated in favor of the discrete unknowns by imposing boundary conditions on cell surfaces normal to the independent variable. A set of discrete equations is obtained by imposing continuity of each variable (and its derivative for the second-order ODEs) at cell interfaces. This process leads to a set of 15 coupled, algebraic equations per cell for $\bar{u}^{yzt}_{ijk}$, $\bar{v}^{yzt}_{ijk}$, $\bar{w}^{yzt}_{ijk}$, $\bar{p}^{yzt}_{ijk}$, $\bar{u}^{zxt}_{ijk}$, $\bar{v}^{zxt}_{ijk}$, $\bar{w}^{zxt}_{ijk}$, $\bar{p}^{zxt}_{ijk}$, $\bar{u}^{xyt}_{ijk}$, $\bar{v}^{xyt}_{ijk}$, $\bar{w}^{xyt}_{ijk}$, $\bar{p}^{xyt}_{ijk}$, $\bar{u}^{xyz}_{ijk}$, $\bar{v}^{xyz}_{ijk}$, and $\bar{w}^{xyz}_{ijk}$ in terms of the 15 pseudosource terms S's.

II.D. Constraint Equations

Following the procedures for the NIM, the pseudosource terms are eliminated next using 15 constraint equations. Four constraint equations are obtained by applying the operator,

$$\frac{1}{16 a_i b_j c_k \tau_n} \int_{-\tau_n}^{\tau_n} \int_{-c_k}^{c_k} \int_{-b_j}^{b_j} \int_{-a_i}^{a_i} dx dy dz dt \ ,$$

on Eqs. (7) through (10). The other 11 constraint equations are obtained by imposing the condition that the cell-averaged variables be unique, independent of the order of integration.[1] Hence, for example, for the cell-averaged u velocity,

$$\begin{aligned} \frac{1}{2a_i} \int_{-a_i}^{a_i} \bar{u}^{yzt}(x)\, dx &= \frac{1}{2b_j} \int_{-b_j}^{b_j} \bar{u}^{zxt}(y)\, dy \\ &= \frac{1}{2c_k} \int_{-c_i}^{c_i} \bar{u}^{xyt}(z)\, dz \\ &= \frac{1}{2\tau_n} \int_{-\tau_n}^{\tau_n} \bar{u}^{xyz}(t)\, dt \ . \end{aligned} \tag{30}$$

The pseudosource terms in the set of discrete algebraic equations are eliminated using these constraint equations leading to a final set of 15 equations and 15 unknowns per cell.

II.E. Boundary Conditions

Boundary conditions for the 3-D MNIM (Ref. 10) are similar to those developed for the 2-D MNIM (Ref. 5). No slip boundary conditions are imposed on solid surfaces. In addition, the Dirichlet condition can also be specified, for example, on inlet surfaces. Boundary conditions for pressure on no-slip surfaces for the 3-D case are derived using the x, y, and z momentum equations.[11] For example, on the no-slip surface at $x = x_{max}$, $u = v = w = 0$, $\partial u/\partial t = \partial^2 u/\partial y^2 = \partial^2 u/\partial z^2 = 0$, and thus, the u-momentum equation, averaged locally over y, z, and t, becomes (see Fig. 1)

$$\frac{1}{\rho} \frac{d\bar{p}^{yzt}(x)}{dx} - \upsilon \frac{d^2 \bar{u}^{yzt}(x)}{dx^2} + \bar{b}_x^{yzt} = 0 \ . \tag{31}$$

Using Taylor expansion and imposing the continuity equation on the no-slip surface at $x = x_{max}$, the following expression with second-order accuracy for $d^2\bar{u}^{yzt}/dx^2$ can be derived:

$$\left.\frac{d^2\bar{u}^{yzt}}{dx^2}\right|_{wall} = \frac{d^2\bar{u}^{yzt}(x=x_0)}{dx^2} = -\frac{2(3h_1^2+3h_1h_2+h_2^2)}{h_1^2(h_1+h_2)^2}\,\bar{u}^{yzt}_{i,j} + \frac{2(h_1+h_2)}{h_1^2h_2}\,\bar{u}^{yzt}_{i-1,j} - \frac{2h_1}{h_2(h_1+h_2)^2}\,\bar{u}^{yzt}_{i-2,j} + O(h^2)\ . \tag{32}$$

A second-order accurate scheme for the first derivative of pressure at the wall has the following form:

$$\left.\frac{d\bar{p}^{yzt}}{dx}\right|_{wall(x=x_0)} = \frac{\bar{p}^{yzt}_{i,j,k} - \bar{p}^{yzt}_{i-1,j,k}}{h_1} + \frac{\bar{p}^{yzt}_{i,j,k}h_2 - \bar{p}^{yzt}_{i-1,j,k}(h_1+h_2) + \bar{p}^{yzt}_{i-2,j,k}h_1}{h_2(h_1+h_2)} + O(h^2)\ . \tag{33}$$

These expressions for $d^2\bar{u}^{yzt}/dx^2$ and $d\bar{p}^{yzt}/dx$ are substituted in Eq. (31) to obtain the discrete form of the pressure boundary condition for $\bar{p}^{yzt}_{i,j,k}$ on the wall at $x = x_{max}$. Pressure boundary conditions for the other walls are similarly derived.

II.F. New Features of the Modified Nodal Integral Method

As in the 2-D MNIM, three characteristics of the numerical scheme differentiate the MNIM from the conventional NIM. First, the local solution of transverse-averaged velocities has a component that varies exponentially in space. These exponential terms can capture a steep spatial variation of velocities within each cell, thus allowing the use of coarse meshes. Second, because of the appearance of the local Reynolds number in the exponential terms, the scheme developed here has inherent upwinding. Moreover, the local Reynolds number, based only on *previous* time step velocities, appears as an argument of the exponential terms. Hence, these terms can be evaluated at the beginning of each time step outside the iteration loop, which significantly reduces the computation time. Third, local transverse-integrated velocities in *all* directions have the same *constant* + *linear* + *exponential* functional form. Hence, unlike the NIM, the MNIM leads to a set of discrete equations that are *symmetric* in *x*, *y*, and *z* directions.

II.G. Code Implementation of the Modified Nodal Integral Method

This set of equations has been implemented in a FORTRAN code and tested on several 3-D fluid flow problems. Steady-state problems are solved by marching in time. Several iterative approaches have been tested to solve the final set of algebraic equations at each time step. Results presented are based on a SIMPLE-like algorithm.[12] Gauss-Seidel iterations are used for each field variable. That is, for a fixed pressure field, velocities are evaluated row by row over the whole domain. Next, keeping velocities fixed, discrete pressure values are evaluated row by row over the entire domain. For a given velocity field, about 15 pressure sweeps yield near-optimum convergence. As is the case with many other

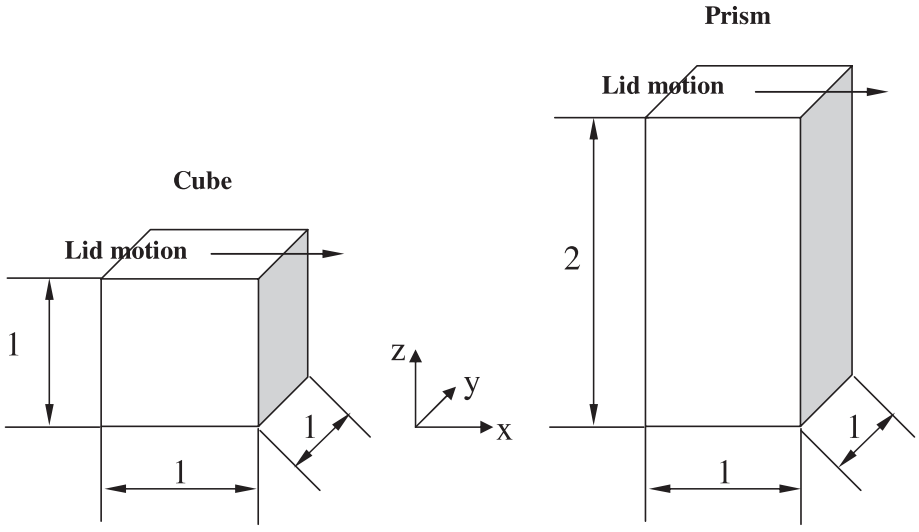

Fig. 2. Configuration of the lid-driven cavity problem.

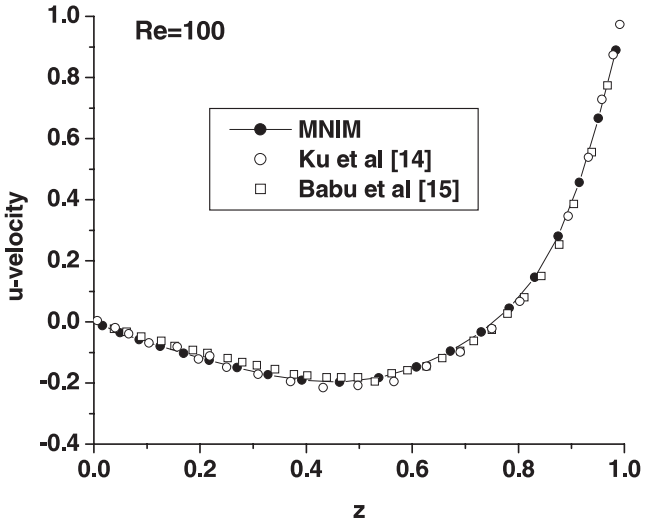

Fig. 3. The u-velocity along the vertical centerline for the 3-D lid-driven cavity problem in a cube for Re = 100.

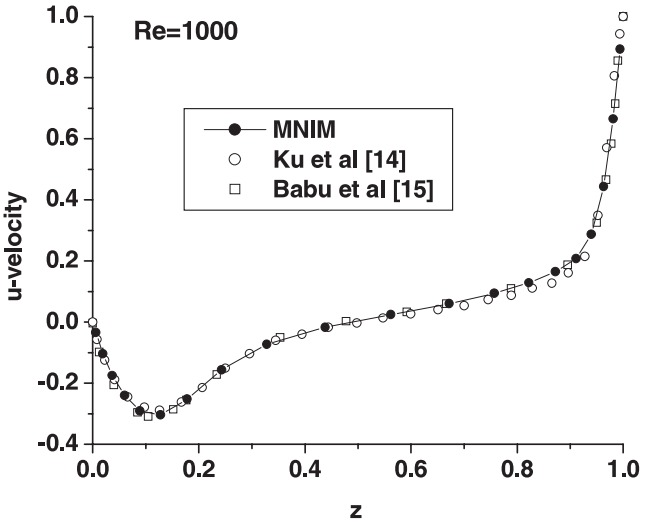

Fig. 5. The u-velocity along the vertical centerline for the 3-D lid-driven cavity problem in a cube for Re = 1000.

iterative approaches, for a given pressure field, only a single sweep to update the velocity was found to be sufficient.

III. NUMERICAL RESULTS

Here, we report the results for the 3-D, lid-driven cavity problems,[13–16] in which the lid at the top ($z = 1$ for a cube and $z = 2$ for a prism) moves with a constant velocity in the x direction (see Fig. 2). Figures 3 and 4 illustrate the u and w velocities in the cube along the centerline parallel to the z axis and x axis, respectively, for a Reynolds number of 100. Figures 5 and 6 are corresponding velocity profiles for a Reynolds number of 1000. These results are obtained using a $20 \times 20 \times 20$ nonuniform mesh and are compared with those from Refs. 14 and 15. It is clear from these results that even for coarse meshes, the MNIM for the time-dependent N-S equations leads to fairly accurate results. For the Re = 1000 case, Babu and Korpela[15] used an $81 \times 81 \times 81$ mesh, while a $20 \times 20 \times 20$ mesh is used in the MNIM. The MNIM code takes ~60 min for Re = 100

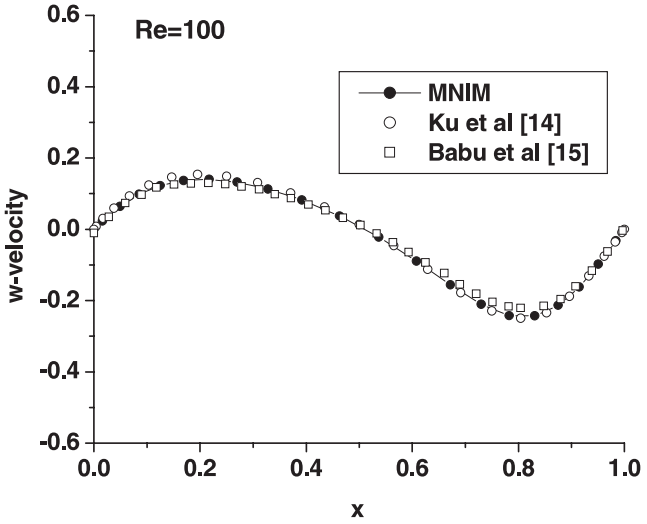

Fig. 4. The w-velocity along the horizontal centerline for the 3-D lid-driven cavity problem in a cube for Re = 100.

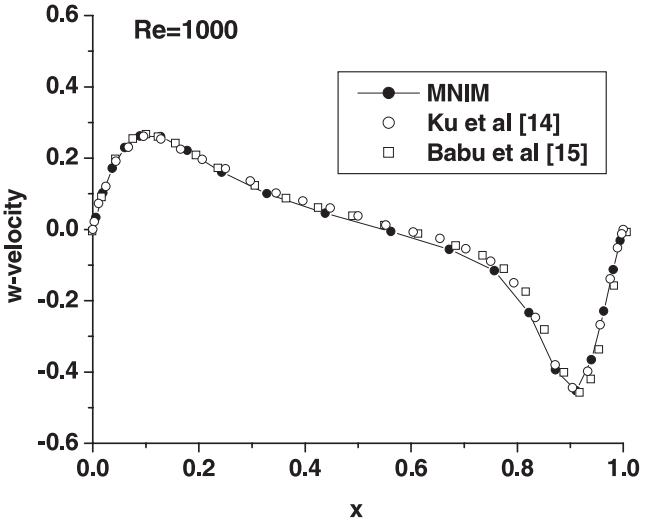

Fig. 6. The w-velocity along the horizontal centerline for the 3-D lid-driven cavity problem in a cube for Re = 1000.

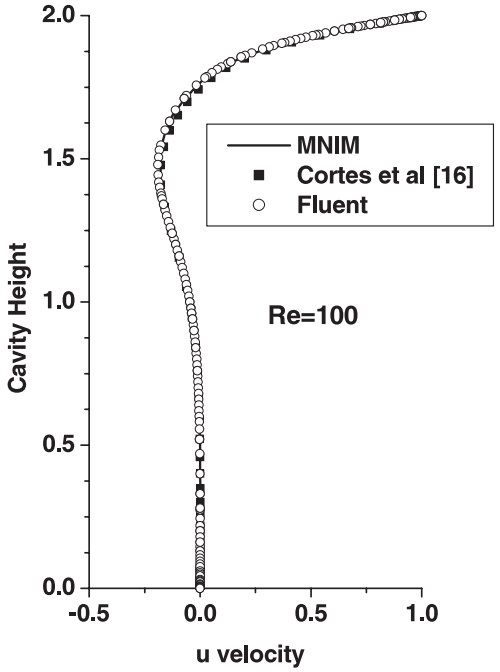

Fig. 7. Comparison of centerline velocity profiles in a prismatic cavity with an aspect ratio of 2 for Reynolds number of 100.

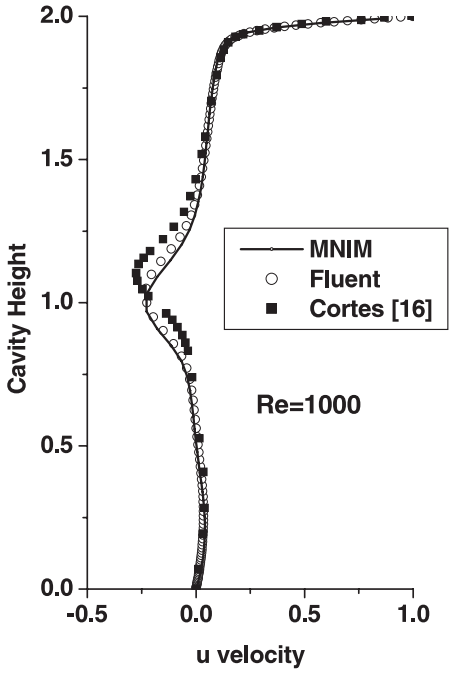

Fig. 8. Comparison of centerline velocity profiles in a prismatic cavity with an aspect ratio of 2 for Reynolds number of 1000.

and 126 min for Re = 1000 on a 1.5-GHz personal computer running a LINUX operating system. The CPU time for this 3-D problem is low despite the fact that very simple Gauss-Seidel sweeps are used repeatedly at each time step until convergence. For larger problems, significant savings in CPU time can be achieved by incorporating more efficient solvers.

In the prism case, a $20 \times 20 \times 40$ nonuniform mesh with a geometric factor of 1.1 was used for a Reynolds number of 100 for the MNIM. The MNIM results agree very well with the reference solution (see Fig. 7), which was obtained using a $35 \times 35 \times 70$ mesh.[16] A time step of 0.03 was used, and steady state was reached after 300 time steps. The reference solution[16] on the other hand was obtained using time steps of 0.00025 and 60 000. These results also match results obtained on a very fine mesh using the FLUENT commercial software.

For flow in the prism with a Reynolds number of 1000, numerical results obtained using the MNIM on a $30 \times 30 \times 60$ mesh agree very well with results obtained using FLUENT with a denser $60 \times 60 \times 120$ mesh (see Fig. 8). However, both results differ somewhat in the middle portion of the cavity from those reported in Ref. 16 obtained using a $35 \times 35 \times 70$ mesh (see Fig. 8). Though it is difficult to conclude with certainty which of the two solutions in the middle part of the cavity is the correct one, agreement between results obtained using the MNIM and FLUENT suggests that the mesh used in Ref. 16 may still be too coarse for the numerical scheme.

IV. SUMMARY

An MNIM for 3-D, time-dependent N-S equations is developed. It is an extension of the 2-D scheme reported recently. Results obtained using the modified scheme are compared with those reported in literature for 3-D lid-driven cavity problems in cube- and prism-shaped cavities. Good agreement is found between results obtained here and reference solutions. Moreover, the grid size used in the MNIM is much coarser than those used earlier to solve these same problems.

ACKNOWLEDGMENTS

Research funded in part by the U.S. Department of Energy through the University of California under subcontract B341494. First author (FW) would also like to acknowledge support under the Computational Science and Engineering Fellowship program at University of Illinois at Urbana Champaign.

REFERENCES

1. Y. Y. AZMY and J. J. DORNING, "A Nodal Integral Approach to the Numerical Solution of Partial Differential

Equations," *Advances in Reactor Computations*, Vol. II, p. 893, American Nuclear Society, La Grange Park, Illinois (1983).

2. G. L. WILSON, R. A. RYDIN, and Y. Y. AZMY, "Time-Dependent Nodal Integral Method for the Investigation of Bifurcation and Nonlinear Phenomena in Fluid Flow and Natural Convection," *Nucl. Sci. Eng*., **100**, 414 (1988).

3. P. D. ESSER and R. J. WITT, "An Upwind Nodal Integral Method for Incompressible Fluid Flow," *Nucl. Sci. Eng*., **114**, 20 (1993).

4. E. P. E. MICHAEL and J. J. DORNING, "A Primitive-Variable Nodal Method for Steady-State Fluid Flow," *Trans. Am. Nuc. Soc*., **83**, 420 (2000).

5. F. WANG and RIZWAN-UDDIN, "A Modified Nodal Scheme for the Time-Dependent, Incompressible Navier-Stokes Equations," *J. Comput. Phys*., **187**, 168 (2003).

6. R. D. LAWRENCE, "Progress in Nodal Methods for the Solutions of the Neutron Diffusion and Transport Equations," *Prog. Nucl. Energy*, **17**, *3*, 271 (1986).

7. A. J. TOREJA and RIZWAN-UDDIN, "Hybrid Numerical Methods for the Convection-Diffusion Equation in Arbitrary Geometries," *Proc. Int. Conf. Mathematics and Computation, Reactor Physics and Environmental Analysis in Nuclear Applications (M&C-99)*, Madrid, Spain, September 27–30, 1999, p. 1705, J. M. ARAGONES, Ed., Senda Editorial (1999).

8. J. C. TANNEHILL, D. A. ANDERSON, and R. H. PLETCHER, *Computational Fluid Mechanics and Heat Transfer*, 2nd ed., Taylor and Francis (1997).

9. K. N. GHIA, W. L. HANKEY, Jr., and J. K. HODGE, "Study of Incompressible Navier-Stokes Equations in Primitive Variables Using Implicit Numerical Technique," AIAA Paper 77-648, American Institute of Aeronautics and Astronautics (1977).

10. F. WANG and RIZWAN-UDDIN, "Pressure Boundary Conditions for Modified Nodal Integral Method for Incompressible Navier-Stokes Equations," *Trans. Am. Nucl. Soc*., **89**, 332 (2003).

11. J. C. TANNEHILL, D. A. ANDERSON, and R. H. PLETCHER, *Computational Fluid Mechanics and Heat Transfer*, 2nd ed., Taylor and Francis (1997).

12. S. V. PATANKAR, *Numerical Heat Transfer and Fluid Flow*, Hemisphere (1980).

13. A. BALOCH, P. W. GRANT, and M. F. WEBSTER, "Homogeneous and Heterogeneous Distributed Cluster Processing for two and Three-Dimensional Viscoelastic Flows," *Int. J. Numer. Methods Fluids*, **40**, 1347 (2002).

14. H. C. KU, R. S. HIRSH, and T. D. TAYLOR, "A Pseudospectral Method for Solution of the Three-Dimensional Incompressible Navier-Stokes Equations," *J. Comput. Phys*., **70**, 439 (1987).

15. V. BABU and S. A. KORPELA, "Numerical Solution of the Incompressible, Three-Dimensional Navier-Stokes Equations," *Comput. Fluids*, **23**, 675 (1994).

16. A. B. CORTES and J. D. MILLER, "Numerical Experiments with the Lid Driven Cavity Flow Problem," *Comput. Fluids*, **23**, 1005 (1994).